ГИАБ. Горный информационно-аналитический бюллетень /
MIAB. Mining Informational and Analytical Bulletin, 2019;(10):117-130

УДК 552.541:552.08 DOI: 10.25018/0236-1493-2019-10-0-117-130

ОСОБЕННОСТИ ВОЗДЕЙСТВИЯ ПОСЛЕДОВАТЕЛЬНЫХ ПЕРИОДИЧЕСКИХ ДВУХОСНЫХ ЦИКЛИЧЕСКИХ НАГРУЖЕНИЙ НА ПРОЧНОСТЬ И АКУСТИЧЕСКИЕ СВОЙСТВА ИЗВЕСТНЯКОВ

А.С. Вознесенский[1], М.Н. Красилов[1], Я.О. Куткин[1], М.Н. Тавостин[2]

[1] НИТУ «МИСиС», Москва, Россия, e-mail: al48@mail.ru
[2] ООО «Газпром геотехнологии», Москва, Россия

Аннотация: Представлены результаты экспериментов, направленных на оценку влияния последовательных циклических воздействий в одном и двух направлениях на прочность и акустические свойства образцов известняка Касимовского месторождения. В качестве информативных параметров использовались скорости упругих продольных и поперечных волн, добротность, динамический модуль упругости и прочность. Наибольшие изменения информативные параметры испытывают при числе циклов до 50—100, а затем происходит их стабилизация. Анализ зависимостей прочности от количества циклов *M* показывает на ее снижение на первых 50 циклах нагружений, а при большем количестве *M* наблюдается стабилизация. При этом прочность образцов, подвергавшихся воздействиям по двум направлениям, оказалась выше, чем у образцов, нагружаемых по одному направлению. Полученные зависимости акустических параметров от количества циклов *M* аппроксимируются экспоненциальными функциями вида $y = a_0 + a_1\exp(-x/a_2)$. Регистрация нагрузки и продольных деформаций образцов позволила рассчитать изменения дифференциального модуля деформаций E_d. Характер изменения кривых дифференциального модуля деформаций E_d при одноосном циклическом нагружении отличается плавным его возрастанием и последующим нарастанием с постоянной скоростью, в то время как скорость роста E_d при повторном нагружении в перпендикулярном направлении существенно ниже, чем при первом. Изменения при первом нагружении находятся в пределах 2—10%, а при двухосном гораздо ниже — в пределах 1,5—2%. При использовании полученных результатов на практике может быть рекомендовано использование по возможности двух- или многоосных циклических нагружений в случае, когда задачей является сохранение прочности, и одноосных нагружений, когда необходимо наиболее быстрое ее уменьшение.

Ключевые слова: горные породы, усталость, прочность, закономерности, влияние, циклический, воздействие, акустический, свойства, деформации.

Благодарность: Исследование выполнено при финансовой поддержке РФФИ в рамках научно-исследовательского проекта № 17-05-00570.

Для цитирования: *Вознесенский А. С., Красилов М. Н., Куткин Я. О., Тавостин М. Н.* Особенности воздействия последовательных периодических двухосных циклических нагружений на прочность и акустические свойства известняков // Горный информационно-аналитический бюллетень. – 2019. – № 10. – С. 117–130. DOI: 10.25018/0236-1493-2019-10-0-117-130.

© А.С. Вознесенский, М.Н. Красилов, Я.О. Куткин, М.Н. Тавостин. 2019.

Peculiarities of the impact of consecutive periodic biaxial cyclic loading on the strength and acoustic properties of limestone

A.S. Voznesenskii[1], M.N. Krasilov[1], Ya.O. Kutkin[1], M.N. Tavostin[2]

[1] National University of Science and Technology «MISiS», Moscow, Russia, e-mail: al48@mail.ru
[2] LLC «Gasprom geotechnology», Moscow, Russia

Abstract: This article presents the experimental findings to assess the consecutive series of cyclic impact in one and two directions of axial compression on the strength and acoustic properties of limestone samples collected in the Kasimov Field. The velocities of elastic longitudinal and transverse waves, acoustic quality factor (*Q*-factor), dynamic elasticity modulus, and strength were used as information-bearing parameters. The information-bearing parameters vary greatly at the range of 50—100 loading cycles, and then they normalize. Analysis of the strength's dependence on the number of cycles *M* indicates its decrease during the first 50 cycles of loading, whereby the strength normalizes as the *M* value rises. At that, the strength of samples exposed to impact in both directions was higher than that of the samples loaded in one direction. The obtained dependences of acoustic parameters on the number of cycles *M* are approximated by the exponential functions of $y = a_0 + a_1\exp(-x/a_2)$. Recording the load and the sample longitudinal deformation helped calculate the variations of the differential modulus of deformation E_d. The behavior of the E_d curve at the uniaxial cyclic loading is distinguished by its smooth ascendancy and subsequent increment at a constant speed. The E_d growth rate at re-loading in the perpendicular direction is significantly lower than at the first loading direction. variations during the first loading range from 2 to 10%, and these variations are lower under biaxial loading, which are 1,5 to 2%. When these findings are applied in practice, the bi- or multi-axial cyclic loadings may be recommended for use where the goal is to retain the strength. In turn, the uniaxial loadings may be recommended where the fastest strength reduction is required.

Key words: Rocks, fatigue, strength, regularities, influence, cyclic, impact, acoustic, properties, deformation.

Acknowledgements: The reported study was funded by RFBR according to the research project No 17-05-00570.

For citation: Voznesenskii A. S., Krasilov M. N., Kutkin Ya. O., Tavostin M. N. Peculiarities of the impact of consecutive periodic biaxial cyclic loading on the strength and acoustic properties of limestone. *MIAB. Mining Inf. Anal. Bull.* 2019;(10):117-130. [In Russ]. DOI: 10.25018/0236-1493-2019-10-0-117-130.

Introduction

Fatigue cyclic loadings of the rock occur in a range of transport, construction and mining facilities, e.g. rock in crushing [1, 2], drilling [3, 4], or explosion operations [5, 6]; rock mass around mine workings [7], aggregates in the reinforced concrete and asphalt concrete, crushed stone in railway beds when exposed to the moving transport [8, 9]; rock mass to which mast and wind power plants foundations are fastened under the impact of wind [10], etc. Therefore, we understand the concern of researchers who study the rock behavior under cyclic loading which is shown in detail in [11, 12]. Under such impacts, rocks are exposed to the multi-axial force impacts that weaken the rock strength. The result of multi-axial impact may differ from impact occurring in a single direction. Yet, the multi-axial fatigue effect both in metals [13] and rocks [14, 15] is the subject of numerous publications. In practice, the problem often arises of non-destructive testing of the rock strength and evaluating its changes due to multi-axial cyclic loading. To solve various problems during the rock

investigation, and, in particular, strength analysis, commonly used techniques include acoustic methods among which the measurements of velocities and attenuation of elastic waves [16], as well as the acoustic emission method [17, 18] are widespread. In that respect, the critical task is to study the features of multi-axial impact on the rock strength and acoustic properties. The task is specified based on the practical purpose, when the rock strength calls for retention in certain cases or needs to be reduced as fast as possible in other cases.

The authors of this paper conducted a range of studies to test the fatigue of different types of rocks exposed to the cyclic uniaxial compression and tension [19, 20]. The studies focused on the non-destructive strength testing per the obtained regression dependences on acoustic quality factor (Q-factor). This paper is the continuation of the works above.

The results described below were obtained in a study aiming comparative assessment of the impact on the rock strength and the acoustic properties of consecutive series of cyclic force in one and two directions.

Rock samples, experimental equipment and test methods

For the purpose of the study, the limestone samples were taken from the Kasimov Field (Ryazan region, Russia) sized 25×50×50 mm. The samples were tested in pairs: one sample in the series of M loads was tested on one axis, another one — in two consecutive series of $M/2$ loads in normal directions along long axes. Designations of samples and test types are given in Table 1.

The samples were labeled with the following:

- a sample number assigned during the preparation works;
- a number of loading directions 1 or 2;
- the total number of loading cycles M: 50, 75, 100, 125, 150;
- the number of the sub-series 1 or 2, if the loading was applied in two normal directions, $M/2$ loadings in each sub-series. Therefore, a sample tested in 50 loads in one direction was marked as LM_3_11_1_50, as for two directions — it was marked as LM_3_11_2_50. The data on the sample tested in two directions were marked as LM_3_11_2_50(1) and LM_3_11_2_50(2), where in brackets the number of sub-series was indicated corresponding to the load direction. A total of 10 samples were tested, of which 5 were loaded in one direction and 5, in two directions. With the odd total number of cycles in the series for biaxial test specimens, the number of cycles in each sub-series increased to the nearest integer. For example, for M = 75 the number of cycles in the sub-series was 38. Five more samples were tested at the beginning of the test to

Table 1

List of samples and data groups for uniaxial and biaxial testing
Перечень образцов и групп данных при одноосных и двухосных испытаниях

No. of cycles	Uniaxial	Biaxial	
	First series	First series	Second series
50	LM_3_11_1_50	LM_3_11_2_50(1)	LM_3_11_2_50(2)
75	LM_3_12_1_75	LM_3_12_2_75(1)	LM_3_12_2_75(2)
100	LM_3_9_1_100	LM_3_9_2_100(1)	LM_3_9_2_100(2)
125	LM_3_7_1_125	LM_3_7_2_125(1)	LM_3_7_2_125(2)
150	LM_3_17_1_150	LM_3_15_2_150(1)	LM_3_15_2_150(2)

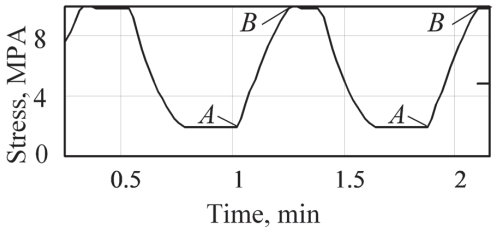

Fig. 1. Reference points of load and deformation curves under cyclic tests for the identification of the differential elasticity modulus

Рис. 1. Расчетные точки кривых нагружения и деформаций при циклических испытаниях для определения дифференциального модуля упругости

define the average compressive strength value.

Cyclic loading was applied via the ASIS universal test equipment (NPP GEOTEK LLC, Penza). The acoustic emission (AE) in the frequency band of 20 kHz to 2 MHz was registered using the AF—15 device and the QMBox modular measurement system (Scientific and Production Group «R-technologies», Moscow). Acoustic Q-factor measurements were taken using the customized laboratory equipment [21]. The velocities of longitudinal and transverse elastic waves were measured using the «Ultrasound» device («Ecogeos Prom» LLC, Tver) within a frequency of about 100 kHz.

The test method included:

• preliminary measurements of the acoustic Q-factor and the velocities of longitudinal and transverse elastic waves of all sample pairs;

• definition of the average compressive strength value for 5 samples of limestone;

• tests of sample pairs in series of M = = 50, 75, 100, 125 and 150 cycles under loading in one direction and series of $M/2$ cycles in two directions with the maximum load per cycle equal to 10 MPa (65% of ultimate strength) and a minimum of 2 MPa (10% of the ultimate strength); in this case, during a series of cyclic loads, axial loads and sample deformations were recorded, as well as the activity of AE to be then recalculated in the number of AE pulses;

• the measurement of the acoustic Q-factor and the velocities of longitudinal and transverse elastic waves after each complete series of cyclic loading;

• definition of the tensile strength after a series of cyclic loading.

Axial loads and longitudinal deformations records helped us calculate the differential module of deformations on the straight branch as formulated below:

$$E_d = \frac{\sigma_B - \sigma_A}{\varepsilon_B - \varepsilon_A},$$

where, E_d is the differential deformations module; σ_A, σ_B, ε_A, ε_B are the stresses and relative strains in points A and B, accordingly, as it is seen in Fig. 1.

The single loading cycle time, including two pauses under the highest and lowest load, depended on the loading machine performance and was 40 to 50 seconds.

The elastic wave velocities were measured along the sample long axes, and the transverse wave polarization plane matched the direction of the sample small axis. The measurement directions were indexed as 1 along the initial loading axis and as 2 across that axis, respectively. Measurements of the longitudinal and transverse elastic wave velocities allowed us to calculate the dynamic modulus of elasticity using the formula below:

$$E_{din} = \frac{\rho C_s^2 \left(3C_p^2 - 4C_s^2\right)}{C_p^2 - C_s^2},$$

where, E_{din} is the dynamic modulus of elasticity; ρ is the density; and C_p, C_s are the velocities of the longitudinal and transverse elastic waves.

Results

The results of the acoustic properties measurements are shown in Fig. 2—5. These measurements were taken for each

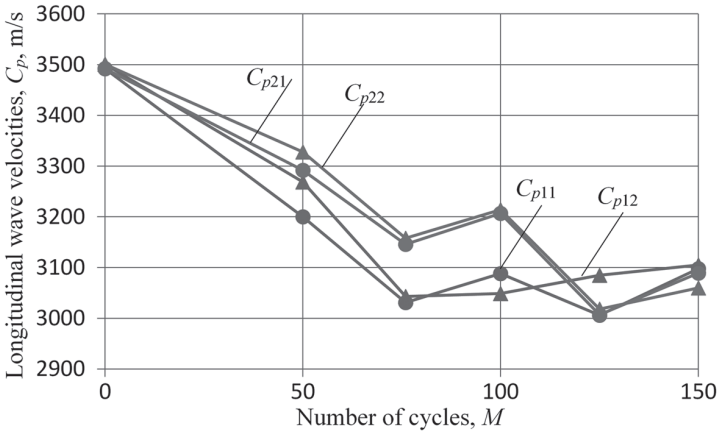

Fig. 2. Dependence graphs of the longitudinal wave velocities C_p on the number of cycles M
Рис. 2. Графики зависимостей скоростей продольных волн C_p от количества циклов M

pair of samples first before the tests, and then after they were completed, based on the given number of loading cycles in the series *M*. After that, the samples were destroyed to measure their strength.

Fig. 2 shows the measured longitudinal velocities of ultrasonic waves depending on the number of loading cycles *M*. The first digit of the index indicates the loading direction. The digit 1 means that all *M* loading/unloading cycles were in one direction, and the digit 2 means that the first *M*/2 loads were in the first direction, and the second ones — in the normal direction. The second digit of the index indicates the direction of the information-bearing parameter measurement. The digit 1 indicates that the measurements were made in the direction of the first loading, while the digit 2 indicated that they were made in the normal direction.

Fig. 3 shows the measurements of transverse elastic wave velocities C_{s11}, C_{s12}, C_{s21}, C_{s22}. They exhibit a gradual decrease as *M* increases, whereas the load velocity values in two directions are usually greater than that of the velocities measured under impact in one direction.

Fig. 4 shows the similar graphs of changes in the acoustic Q-factors Q_1 and Q_2.

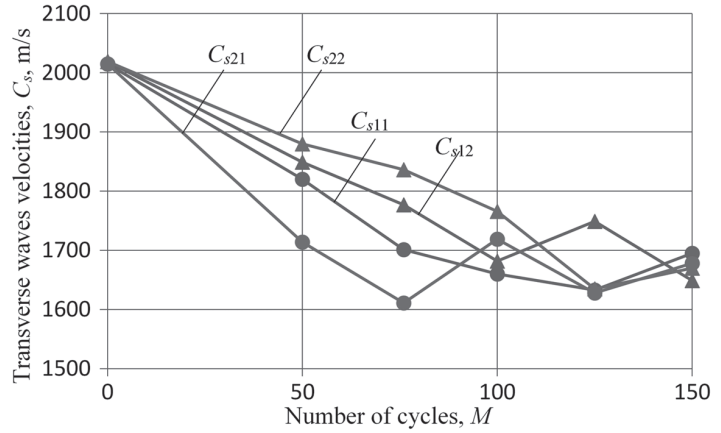

Fig. 3. The measurements of the velocities of transverse elastic waves C_s as per the number of cycles M
Рис. 3. Результаты измерения скоростей поперечных упругих волн C_s от количества циклов M

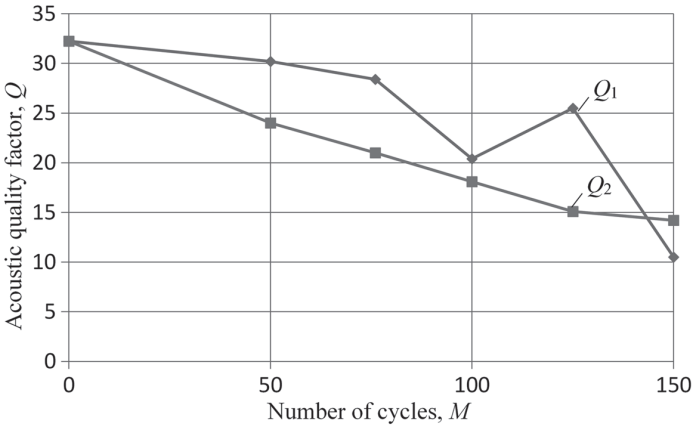

Fig. 4. Measurements of the acoustic Q-factor under uniaxial (Q_1) and biaxial (Q_2) loads on the number of cycles M

Рис. 4. Результаты измерения акустических добротностей при одноосном (Q_1) и двухосном (Q_2) нагружениях от количества циклов M

Q-factor measurements were taken only in the single direction of the first loading. As *M* increases, they decrease as do the velocities. At 150 cycles, this decrease is by 1,8 times for Q_1 and 1,4 times for Q_2.

Fig. 5 shows the graphs of strength variations under uniaxial loading. The greatest strength variations are seen in the initial segment from the beginning and up to 50 cycles. Meanwhile, the strength reduced by 1,3 times. With a higher *M* value, no obvious variations in strength are observable. It should also be noted that the strength under biaxial loading upon exposure was greater than under the uniaxial loading.

Fig. 6 shows the graphs of variations in the dynamic modulus of elasticity under uniaxial and biaxial impacts. They also decreased as *M* went up, while the dynamic module under biaxial loading remained greater than under the uniaxial loading. As *M* raised the impact of the loads on the dynamic modules decreased.

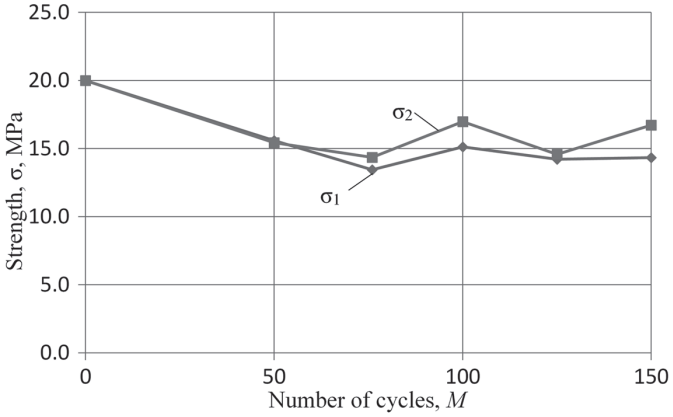

Fig. 5. Measurements of the sample strength under the cyclic loading in one (σ_1) and two (σ_2) directions depending on the number of cycles M

Рис. 5. Результаты измерения прочности образцов после циклических нагружений в одном (σ_1) и в двух (σ_2) направлениях в зависимости от количества циклов M

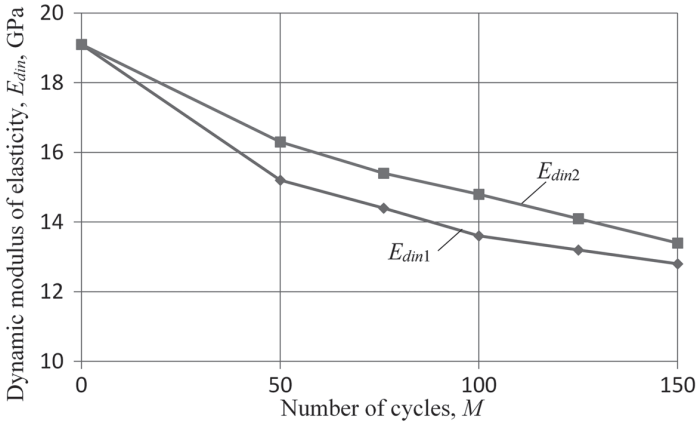

Fig. 6. Measurements of the sample dynamic modulus of elasticity under the cyclic loading in one (E_{din1}) and in two (E_{din2}) directions depending on the number of M cycles

Рис. 6. Результаты измерения динамического модуля упругости образцов после циклических нагружений в одном (E_{din1}) и в двух (E_{din2}) направлениях в зависимости от количества циклов M

Fig. 7 shows an example of load variation graph (a) and longitudinal strain variation graph (b) along with the number of acoustic emission pulses of the LM_3_11_1_50 sample. The number of AE N_Σ showed a significant increase during the first 2—3 cycles, and then the rate of N_Σ increment decreased significantly.

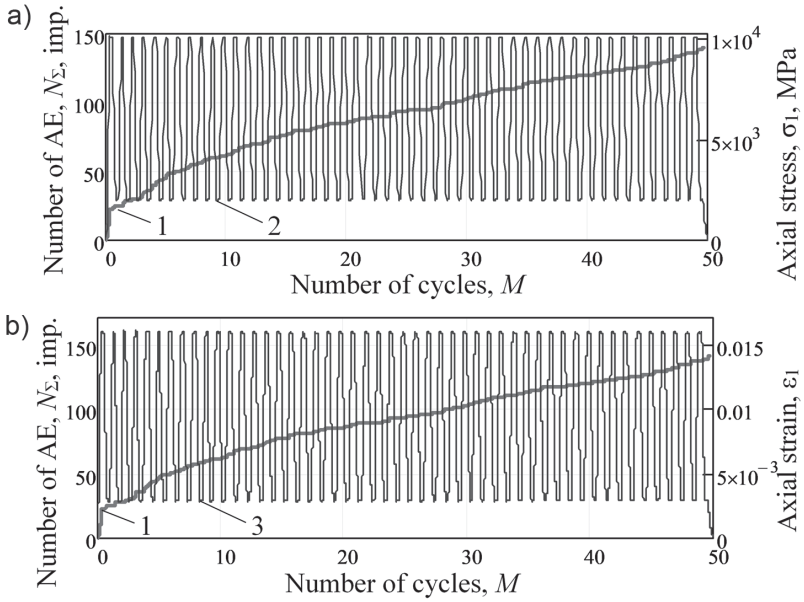

Fig. 7. Dependence graphs of the number of AE N_Σ pulses (curve 1, Fig. a) and stresses σ_1 (curve 2, Fig. a), as well as the number of AE N_Σ pulses (curve 1, Fig. b) and longitudinal strain ε_1 (curve 3, Fig. b) of limestone sample LM_3_11_1_50

Рис. 7. Графики зависимостей числа импульсов АЭ N_Σ (кривая 1, рис. а) и напряжений σ_1 (кривая 2, рис. а), а также числа импульсов АЭ N_Σ (кривая 1, рис. b) и продольных деформаций ε_1 (кривая 3, рис. b) образца известняка LM_3_11_1_50

Discussion

Let us analyze the dependences presented in Fig. 2—7 and first emphasize the qualitative features, before providing quantitative assessments.

First of all, Fig. 5 shows obvious decreases in the strength from 20 to 15 MPa under exposure to the first 50 load/unload cycles. With the number of cycles M exceeding 50, stabilization and minor deviations of strength from 15 MPa are observed. At that, the strength of the samples exposed to biaxial impact is higher than that for samples exposed to loads on one axis. The velocities of both longitudinal and transverse waves in Fig. 2 and Fig. 3 show a decrease as the number of cycles M increases. At the same time, a significant decrease is seen from the beginning of the test to M values within the range of 75 to 100 cycles. Further, their value is lesser secondary to minor deviations from mean values. Thus, it can be noted that the significant impact of cyclic loading affects it velocities only at lower M and then significantly weakens.

The acoustic Q-factor shows similar variation, in particular it decreases, as the number of cycles M increases. However, its behavior differs from uniaxial to biaxial loading. In case of biaxial loading, it shows a smooth decrease as the absolute velocity goes down. It can be assumed that at $M >$ > 150 the direction of the variation curve will be close to horizontal.

The behavior of $Q_1(M)$ curve under uniaxial loading differs from the curve $Q_2(M)$. With a smaller M, the Q-factor reduction of $Q_1(M)$ is minor. The approximating curve $Q_1(M)$ is curved upwards in contrast to the dependences of other information-bearing parameters. This may have to do with the formation of cracks towards the load effect and their weak impact on the quality factor due to a slight decrease in the cross sectional area. As they accumulate to a certain threshold, they impact to a greater extent to result in the more abrupt decrease in the curve. When exposed to a load in two directions, cracks are also formed in two directions as well, which reduces the effective cross-sectional area and has a greater impact on the quality factor. The $Q_2(M)$ curve decreases as early as under the first cycles of impact.

It is seen from the study that the information-bearing parameters are very greatly at the number of cycles of up to 50—100, at which point they stabilize. Such a parameter, as the number of acoustic emission pulses, increases considerably during the first 2—3 cycles, after which it slowly increases at the relatively low velocity of 1—3 impulse/cycle and its increase

Table 2

Approximated dependences of information-bearing parameters on the number of cycles of fatigue uniaxial loading

Результаты аппроксимации зависимостей информативных параметров от количества циклов усталостного одноосного нагружения

Parameter	C_{p11}, m/s	C_{s11}, m/s	E_{din11}, GPa	C_{p12}, m/s	C_{s12}, m/s	E_{din12}, GPa	Q_1*	σ_1**, MPa
a_0	3037	1625	12,58	3047	1578	12,82	32,15	14,25
a_1	458,0	396,1	6,447	461,8	442,6	6,277	–0,7395	5,768
a_2	36,99	54,02	40,41	43,03	93,53	51,32	–45,28	26,84
R^2	0,920	0,944	0,970	0,895	0,935	0,953	0,710	0,926
D^2	11 570	5691	0,883	1690	5760	1,218	93,12	2,050
SD	40,65	28,51	0,36	49,14	28,69	0,420	3,650	0,680

* Dependence differs from dependences on other parameters
** Strength in the first direction

Table 3

Approximated dependences of information-bearing parameters on the number of cycles of fatigue biaxial loading

Результаты аппроксимации зависимостей информативных параметров от количества циклов усталостного двухосного нагружения

Parameter	C_{p11}, m/s	C_{s11}, m/s	E_{din11}, GPa	C_{p12}, m/s	C_{s12}, m/s	E_{din12}, GPa	Q_1	σ_1**, MPa
a_0	2929	1666	13,07	2718	567,9	8,231	2,785	15,21
a_1	566,0	348,0	5,935	787,9	1455	10,92	29,49	4,794
a_2	98,59	24,88	24,79	163,3	489,3	167,7	152,3	12,60
R^2	0,892	0,958	0,883	0,914	0,948	0,905	0,997	0,902
D^2	15 731	4138	3,638	13 836	5228	2,856	0,700	2,061
SD	47,41	24,31	0,720	44,46	27,33	0,640	0,320	0,540

** Strength in the first direction

is not recorded. That is, the process of sample destruction and plastic deformation accumulation at the given level of maximum load level is relatively slow, and the sample deformation mainly occurs in the elasticity area. Material fatigue, which results mainly in case of elastic deformation, is a multi-cycle fatigue [22].

Tables 2 and 3 show the approximation results of the obtained dependences of informative acoustic parameters on the number of cycles M by exponential functions of type $y = a_0 + a_1\exp(-x/a_2)$. Approximation accuracy estimates are provided as well. In these tables R^2 is the determination coefficient and D^2 and *SD* denote the dispersion and the standard deviation, respectively.

In these tables, the a_2 parameter is of interest, which, in this case, shows the number of cycles of readings stabilization in exponential dependence. For information-bearing parameters obtained under the biaxial impact, its value is usually greater than that of the uniaxial impact. It indicates that the information-bearing parameter curves corresponding to the biaxial loading are plotted higher at the same initial values than for uniaxial loading. This is to say, the biaxial impact on their reduction is lower than uniaxial impact. The initial values of the information-bearing parameters at $M = 0$ are estimated as the sum of the coefficients $a_0 + a_1$.

Recording the sample load and longitudinal deformation helped us calculate the variations in the differential modulus of deformation E_d, shown in Table 4.

Comparison of the data in the Table 4 in columns 3 and 4 that describe the differential modulus of deformation of the

Table 4

Values of the differential deformation modulus E_d at the first loading cycle

Значения дифференциального модуля деформаций E_d при первом цикле нагружений

Cycles	Deformation modulus, GPa		
	Direction 1	Direction 2_1	Direction 2_2
1	2	3	4
50	30,8	45,4	45,9
75	53,4	38,3	44,7
100	52,0	46,8	58,4
125	49,5	35,4	37,0
150	49,5	54,4	54,7

same sample, but measured in different directions, allowed us to conclude that the value, in the case of the second direction deformation is normally greater than that of the first direction. Hence, the impact during the first load resulted in the sample's compaction and in the increase in its rigidity and deformation modulus.

Dependences of variations of the differential deformation modulus for different cases are better compared to each other, using relative values. Let's note that the relative deformation modulus below is

$$\xi = E_d / E_{d0},$$

where, E_d and E_{d0} are the current and initial deformation modulus values, respectively. Fig. 8, *a*—*b* show graphs of the ξparameter's variation on *M*.

A difference in the curve behavior during the second biaxial loading (Fig. 8, *c*) draws attention as compared to the uniaxial loading (Fig. 8, *a*) and the first biaxial loading (Fig. 8, *b*). In Fig. 8 *a* and *b*, during the first series of loads for the curves, a smooth increase ξ is observed. During the second series of loads in Fig. 8, *c*, the curves show a sharp growth in the initial part at the number of cycles less than 5 and the subsequent smaller increase in the horizontal direction, even followed by the subsequent decrease in the series of 125 cycles. A significant jump ξ at the

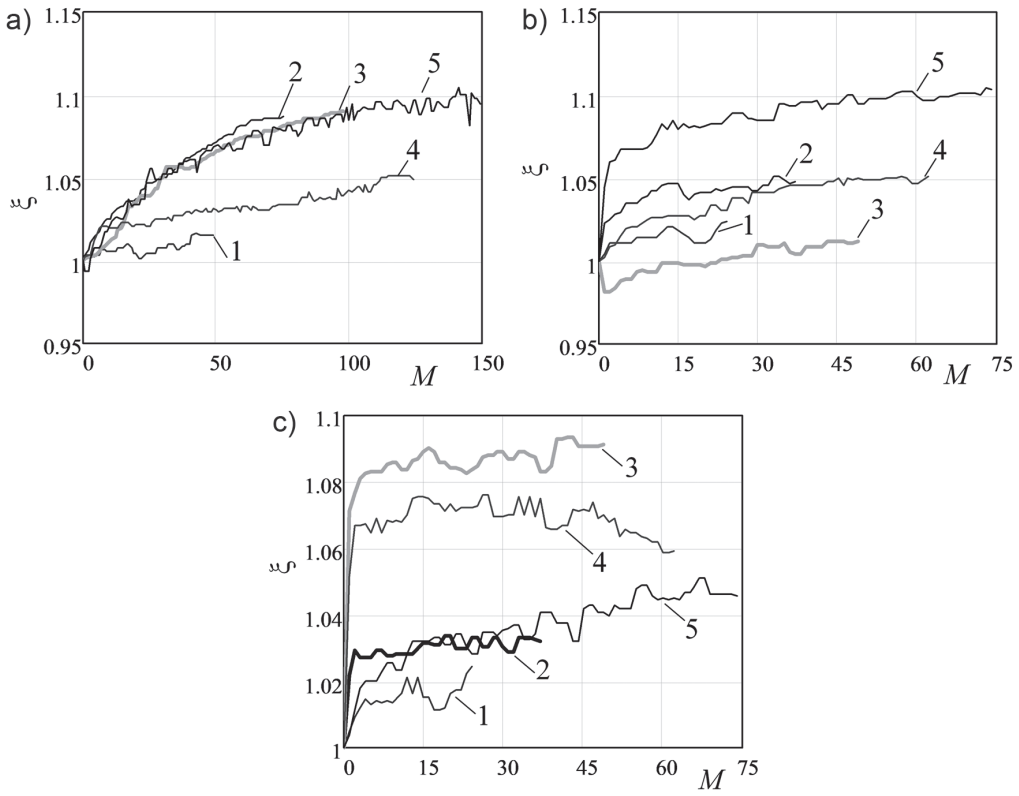

Fig. 8. Dependences of the relative differential deformation modulus ξ for uniaxial (a) and biaxial first (b) and second (c) series of sample loading on the total number of cycles 50 (1), 75 (2), 100 (3), 125 (4), 150 (5)

Рис. 8. Зависимости относительного дифференциального модуля деформаций ξ для случая одноосных (а) и двухосных первых (б) и вторых (в) серий нагружения образцов при общем количестве циклов 50 (1), 75 (2), 100 (3), 125 (4), 150 (5)

beginning of the second loading series is seen at the lesser vertex height of the second loading section compared to the first one. This has to do with the memory effect of the first loading cycle in the series, which increases upon the impact of the previous series of loading in the perpendicular direction.

For an *M* greater than 5 in the first series of loads, the increase in the deformation modulus ranges within 2—10%.

Under the second series of loading for the number of cycles more than 5, the change of the deformation modulus is much less pronounced and does not exceed 1,5—2,0%. Such a minor change in the deformation modulus in that case as shown in Fig. 8, *c*, as compared to that of Fig. 8, *a* and *b*, indicates a greater compaction of the limestone and an increase in its rigidity that occurred during the first series of loading. This is to say, that under the biaxial loading, a denser structure is formed, which also has a greater strength, as is observable in Fig. 5.

The results above show that in case of the same total number of loads, the decrease of informative acoustic parameters relative to *M* under the biaxial loading is less than under the uniaxial loading.

Research limitations and results summary and proposals for practical application

We can make a general conclusion based on the findings that the consecutive biaxial cyclic loading results in a lower level of material destruction as compared to the uniaxial loading.

The obtained results are limited by application of the multi-cycle fatigue mode as formed under the maximum load of 65% of the destruction value. Low-cycle fatigue tests will require further studies.

In assessing the practical application of the findings, one should take into account that the production area needs vary fundamentally from retaining the strength to ensure stability and non-destruction of rock around the working to weakening the strength during the crushing, drilling and explosion works. For preservation of rock strength, biaxial loading may be recommended, and where the strength needs to be reduced — the uniaxial loading is recommended.

Conclusion

1. As the number of limestone sample fatigue loading cycles goes up, the informative parameter variations are shown in the initial decrease and subsequent stabilization of the strength and velocities of elastic waves. The number of acoustic emission pulses upon the significant initial increase shows an abrupt decrease in the increment rate. At the specified maximum load equal to 65% of the strength, sample deformation occurs in the multicycle fatigue mode, when the elastic component is much larger than the plastic component.

2. Successive biaxial loading results in the lesser strength loss than uniaxial loading, which can be attributed to crack formation in two directions. In that case, cracks oriented in one direction prevent crack penetration in the other direction, which leads to greater strength under the periodic fatigue loadings.

3. The curve behavior of the differential deformation modulus E_d under the uniaxial cyclic loading is distinguished by its smooth increase and subsequent increment at a constant rate. The E_d growth rate under loading in the normal direction is significantly lower than under the first loading. Here even the sign changes for the opposite to indicate the significant material compaction that occurred under the first loading and the trend to decompaction under the second loading in the normal direction. Meanwhile, E_d variations

under the first loading range between 2 and 10%, while under the biaxial loading in the normal direction — within 1,5 to 2%.

4. When these findings are applied in practice, the bi- or multi-axial cyclic loadings may be recommended in the case that strength calls to be preserved. Uniaxial loadings may, in turn, be recommended where the rock strength needs be reduced as quickly as possible.

Authors express gratitude to V. Ivanov, P. Dubinin, A. Tyutcheva, A. Luchnikova and R. Nasibullin for their help in designing the laboratory setup and conducting experiments.

Авторы выражают благодарность В. Иванову, П. Дубинину, А. Тютчевой, А. Лучниковой и Р. Насибуллину за помощь в разработке лабораторной установки и проведении экспериментов.

СПИСОК ЛИТЕРАТУРЫ

1. *Виноградов Ю. И.*, *Хохлов С. В.*, *Аникин В. В.* Методика оценки эффективности дробления массива горных пород различными типами ВВ // Известия ТулГУ. Науки о Земле. — 2018. Вып. 2. — С. 214 —221.

2. *Кононенко В. Н.*, *Халкечев К. В.* Резонансное разрушение горных пород при дроблении и измельчении // Горный информационно-аналитический бюллетень. — 2010. — № 1. — С. 231—235.

3. *Синев С. В.* Механизмы, методы и способы разрушения горных пород в шарошечном бурении // Горный информационно-аналитический бюллетень. — 2016. — № 1. — С. 149—159.

4. *Воздвиженский Б. И.*, *Сидоренко А. К.*, *Скорняков А. Л.* Современные способы бурения скважин, 2-е изд., перераб. и доп. — М.: Недра, 1978. — 342 с.

5. *Новиньков А. Г.*, *Протасов С. И.*, *Самусев П. А.* Сейсмическая безопасность подземных горных выработок при ведении взрывных работ на земной поверхности // Безопасность труда в промышленности. — 2018. — № 8. — С. 64—68. DOI: 10.24000/0409-2961-2018-8-64-68.

6. *Викторов С. Д.*, *Закалинский В. М.* Развитие идей совершенствования взрывного разрушения массивов горных пород — основа прогресса в горном деле // Записки Горного института. — 2014. — Т. 210. — С. 30—36.

7. *Тулебаев К. К.* Разрушение свободной поверхности массива горных пород под действием сейсмических волн // Взрывное дело. — 2012. — № 107—64. — С. 289—295.

8. *Celma Cervera C., Jelagin D., Partl M. N, Larsson P. L.* Contact-induced deformation and damage of rocks used in pavement materials. Material Design [Internet]. 2017 Nov [cited 2019 Jun 12]; 133:255-65. Available from: https://linkinghub.elsevier.com/retrieve/pii/S0264127517307499.

9. *Осиновская В. А.* Влияние вибрации нежестких дорожных одежд на их прочность // Интернет-журнал «Науковедение». — № 5 (24), сентябрь — октябрь 2014 [сайт]. URL: http://naukovedenie.ru (дата обращения 10.07.2019).

10. *Руководство* по расчету зданий и сооружений на действие ветра / Центр, науч.-исслед. ин-т строит, конструкций им. В. А. Кучеренко. — М.: Стройиздат, 1978. — 216 с.

11. *Cerfontaine B., Collin F.* (2018) Cyclic and Fatigue Behaviour of Rock Materials: Review, Interpretation and Research Perspectives. Rock Mech Rock Eng 51:391—414. DOI: 10.1007/s00603-017-1337-5.

12. *Braunagel M. J.*, *Griffith W. A.* The Effect of Dynamic Stress Cycling on the Compressive Strength of Rocks. Geophysical Research Letters. 2019. Jun 14. 78. 14. Pp. 416—426.

13. *Papuga J., Fojtík F.* Multiaxial fatigue strength of common structural steel and the response of some estimation methods // International Journal of Fatigue. 2017. 104. Pp. 27—42, DOI: 10.1016/j.ijfatigue.2017.07.001.

14. *Jamali S., Hashemolhosseini H., Baghbanan A., Khoshkam M., Haghgouei H.* Evaluating Fatigue in Crystalline Intact Rocks under Completely Reversed Loading. Geotechnical Testing Journal. Vol. 40. No 5. 2017. Pp. 789—797, DOI: https://doi.org/10.1520/GTJ20160250.

15. *Wang S., Xu W., Sun M., Wang W.* Experimental investigation of the mechanical properties of fine-grained sandstone in the triaxial cyclic loading test. Environmental Earth Science [Internet]. 2019 Jul 16 [cited 2019 Aug 13];78(14):416. Available from: http://link.springer.com/10.1007/s12665-019-8437-3.

16. *Тихоцкий С.А., Фокин И.В., Баюк И.О. и др.* Комплексные лабораторные исследования керна в ЦПГИ ИФЗ РАН // Наука и технологические разработки. — 2017. — Т. 96. — № 2. — С. 17—32.

17. *Shkuratnik V.L., Filimonov Y.L., Kuchurin S.V.* Acoustic-emissive memory effect in coal samples under triaxial axial-symmetric compression. Journal of Mining Science. 2006. 42. No 3. Pp. 203—209.

18. *Damaskinskaya E.E., Panteleev I.A., Gafurova D.R., Frolov D.I.* Structure of a Deformed Inhomogeneous Material on the Data of Acoustic Emission and X-Ray Computer Microtomography 2018, Phys. Solid State, vol. 60, 7. 1363—1367. DOI: http://dx.doi.org/10.1134/S1063783418070077.

19. *Voznesenskii A.S., Krasilov M.N., Kutkin Y.O., Komissarov A.A.* Predicting fatigue strength of rocks by its interrelation with the acoustic quality factor. International Journal of Fatigue. 77. 2015. Pp. 194—198, DOI: 10.1016/j.ijfatigue.2015.02.012.

20. *Voznesenskii A.S., Krasilov M.N., Kutkin Y.O., Tavostin M.N., Osipov Y.V.* Features of interrelations between acoustic quality factor and strength of rock salt during fatigue cyclic loadings. International Journal of Fatigue. — 2017. — 97. — P. 70 —78, DOI: 10.1016/j.ijfatigue.2016.12.027.

21. *Voznesenskii A.S., Kutkin Y.O. Krasilov M.N., Komissarov A.A.* The influence of the stress state type and scale factor on the relationship between the acoustic quality factor and the residual strength of gypsum rocks in fatigue tests. International Journal of Fatigue. 3. 2016, Pp. 53 —58.

22. *ГОСТ 23207-78.* Сопротивление усталости. Основные термины, определения и обозначения. — М.: Изд. стандартов, 1981. — 48 с. ГИАБ

REFERENCES

1. Vinogradov Yu. I., Hohlov S.V., Anikin V.V. Methodology for assessing the effectiveness of crushing a rock massif by various types of explosives. *Izvestiya TulGU. Nauki o Zemle*. 2018. Vyp. 2, pp. 214—221. [In Russ].

2. Kononenko V.N., Halkechev K.V. Resonant destruction of rocks during crushing and grinding. *Gornyy informatsionno-analiticheskiy byulleten'*. 2010, no 1, pp. 231—235. [In Russ].

3. Sinev S.V. Mechanisms, methods and methods of rock destruction in roller drilling. *Gornyy informatsionno-analiticheskiy byulleten'*. 2016, no 1, pp. 149—159. [In Russ].

4. Vozdvizhenskii B.I., Sidorenko A.K., Skornyakov A.L. *Sovremennye sposoby bureniya skvazhin.* 2-e izd. [Modern drilling methods, pp. 2nd edition], Moscow, Nedra, 1978, 342 p.

5. Novinkov A.G., Protasov S.I., Samusev P.A. Seismic safety of underground mining during blasting on the earth's surface. *Labor safety in industry* 2018, no 8, pp. 64—68. DOI: 10.24000/0409-2961-2018-8-64-68. [In Russ].

6. Viktorov S.D., Zakalinskij V.M. The development of ideas for improving the explosive destruction of rock masses is the basis of progress in mining. *Zapiski Gornogo instituta*, 2014. Vol. 210, pp. 30—36. [In Russ].

7. Tulebaev K.K. The destruction of the free surface of a rock mass under the action of seismic waves. *Vzryvnoe delo,* 2012, no 107—64, pp. 289—295. [In Russ].

8. Celma Cervera C., Jelagin D., Partl M.N., Larsson P.L. Contact-induced deformation and damage of rocks used in pavement materials. *Material Design* [Internet]. 2017 Nov [cited 2019 Jun 12]; 133:255-65. Available from: https://linkinghub.elsevier.com/retrieve/pii/S0264127517307499.

9. Osinovskaya V.A. Impact of vibration of non-rigid pavements on their strength. *Online journal «Naukovedenie»*. 2014. No 5. Available at: http://naukovedenie.ru (accessed 10.07.2019). [In Russ].

10. *Rukovodstvo po raschetu zdanii i sooruzhenii na deistvie vetra* [Guide to the calculation of buildings and structures on the action of the wind], Moscow, Stroiizdat, 1978, 216 p. [In Russ].

11. Cerfontaine B., Collin F. Cyclic and Fatigue Behaviour of Rock Materials: Review, Interpretation and Research Perspectives. *Rock Mech Rock Eng*, 2018. 51:391-414. DOI: 10.1007/s00603-017-1337-5.

12. Braunagel M.J., Griffith W.A. The Effect of Dynamic Stress Cycling on the Compressive Strength of Rocks. *Geophysical Research Letters* 2019 Jun 14, 78, 14, pp. 416—426.

13. Papuga, J., Fojtík, F. Multiaxial fatigue strength of common structural steel and the response of some estimation methods. *International Journal of Fatigue* 2017, 104, pp. 27—42, DOI: 10.1016/j.ijfatigue.2017.07.001.

14. Jamali S., Hashemolhosseini H., Baghbanan A., Khoshkam M., Haghgouei H. Evaluating Fatigue in Crystalline Intact Rocks under Completely Reversed Loading. *Geotechnical Testing Journal,* 2017, Vol. 40, no 5, pp. 789—797, DOI: https://doi.org/10.1520/GTJ20160250.

15. Wang S., Xu W., Sun M., Wang W. Experimental investigation of the mechanical properties of fine-grained sandstone in the triaxial cyclic loading test. *Environmental Earth Science* [Internet]. 2019 Jul 16 [cited 2019 Aug 13];78(14):416. Available from: http://link.springer.com/10.1007/s12665-019-8437-3.

16. Tikhotskii S.A., Fokin I.V., Bayuk I.O. Comprehensive laboratory tests of core in CGI IFZ RAS. *Nauka i tekhnologicheskie razrabotki*. 2017, Vol. 96, no 2, pp. 17—32. [In Russ].

17. Shkuratnik V.L., Filimonov Y.L., Kuchurin S.V. Acoustic-emissive memory effect in coal samples under triaxial axial-symmetric compression. *Journal of Mining Science,* 2006, 42, no 3, pp. 203—209.

18. Damaskinskaya E.E., Panteleev I.A., Gafurova D.R., Frolov D.I. Structure of a Deformed Inhomogeneous Material on the Data of Acoustic Emission and X-Ray Computer Microtomography, *Phys. Solid State*, 2018, vol. 60, 7, pp. 1363—1367. DOI: http://dx.doi.org/10.1134/S1063783418070077.

19. Voznesenskii A.S., Krasilov, M. N., Kutkin, Y. O., Komissarov A.A. Predicting fatigue strength of rocks by its interrelation with the acoustic quality factor. *International Journal of Fatigue,* 2015, 77, pp. 194—198, DOI: 10.1016/j.ijfatigue.2015.02.012.

20. Voznesenskii A.S., Krasilov, M. N., Kutkin, Y. O., Tavostin, M. N., Osipov, Y. V. Features of interrelations between acoustic quality factor and strength of rock salt during fatigue cyclic loadings. *International Journal of Fatigue*, 2017, 97, pp. 70—78, DOI: 10.1016/j.ijfatigue.2016.12.027.

21. Voznesenskii A.S., Kutkin Y.O. Krasilov M.N., Komissarov, A. A. The influence of the stress state type and scale factor on the relationship between the acoustic quality factor and the residual strength of gypsum rocks in fatigue tests. *International Journal of Fatigue,* 2016, 3, pp. 53—58.

22. *Soprotivlenie ustalosti. Osnovnye terminy, opredeleniya i oboznacheniya, GOST 23207-78* [Fatigue resistance. Key terms, definitions and designations, State Standart 23207-78], Moscow, Standarty, 1981, 48 p. [In Russ].

ИНФОРМАЦИЯ ОБ АВТОРАХ

Вознесенский Александр Сергеевич[1] — д-р техн. наук, профессор,
e-mail: al48@mail.ru,
Красилов Максим Николаевич[1] — аспирант,
Куткин Ярослав Олегович[1] — канд. техн. наук, доцент,
Тавостин Михаил Николаевич — канд. техн. наук,
старший научный сотрудник, ООО «Газпром геотехнологии»,
[1] НИТУ «МИСиС».
Для контактов: Вознесенский А.С., e-mail: al48@mail.ru.

INFORMATION ABOUT THE AUTHORS

A.S. Voznesenskii[1], Dr. Sci. (Eng.), Professor, e-mail: al48@mail.ru,
M.N. Krasilov[1], Graduate Student,
Ya.O. Kutkin[1], Cand. Sci. (Eng.), Assistant Professor,
M.N. Tavostin, Cand. Sci. (Eng.), Senior Researcher,
LLC «Gasprom geotechnology», 123290, Moscow, Russia,
[1] National University of Science and Technology «MISiS»,
119049, Moscow, Russia.
Corresponding author: A.S. Voznesenskii, e-mail: al48@mail.ru.